

Hands-on Fourier analysis by means of far-field diffraction

This content has been downloaded from IOPscience. Please scroll down to see the full text.

View [the table of contents for this issue](#), or go to the [journal homepage](#) for more

Download details:

IP Address: 149.132.2.57

This content was downloaded on 01/09/2016 at 09:29

Please note that [terms and conditions apply](#).

You may also be interested in:

[Phasor analysis of binary diffraction gratings with different fill factors](#)

Antonio Martínez, Ma del Mar Sánchez-López and Ignacio Moreno

[On the colours of spider orb-webs](#)

Wilfried Suhr and H Joachim Schlichting

[Wave and photon descriptions of light: historical highlights, epistemological aspects and teaching practices](#)

Biagio Buonauro and Giuseppe Giuliani

[Spatial filtering in optical data-processing](#)

K G Birch

[Digital Fourier microscopy for soft matter dynamics](#)

Fabio Giavazzi and Roberto Cerbino

[Understanding the Physical Optics Phenomena by Using a Digital Application for Light Propagation](#)

Daniel-Esteban Sierra-Sosa and Luciano Ángel-Toro

[Laser diffraction microscopy](#)

P Schall

Hands-on Fourier analysis by means of far-field diffraction

Nicolo' Giovanni Ceffa, Maddalena Collini,
Laura D'Alfonso and Giuseppe Chirico

Department of Physics 'G. Occhialini', Università di Milano-Bicocca, Piazza della
Scienza 3, I-20126, Milano, Italy

E-mail: Giuseppe.chirico@unimib.it

Received 18 April 2016, revised 6 July 2016

Accepted for publication 19 July 2016

Published 17 August 2016



CrossMark

Abstract

Coherent sources of light are easily available to university undergraduate laboratory courses and the demonstration of electro-magnetic wave diffraction is typically made with light. However, the construction of arbitrary patterns for the study of light diffraction is particularly demanding due to the small linear scale needed when using sub-micrometer wavelengths, limiting the possibility to thoroughly investigate diffraction experimentally. We describe and test a simple and affordable method to develop arbitrary light diffraction patterns with first year undergraduate or last year high school students. This method is exploited to investigate experimentally the connection between diffraction and the Fourier transform, leading to the development of the concept of spectral analysis of a (2D) signal. We therefore discuss the possibility of building a teaching unit for first year undergraduate or last year high school students on the interdisciplinary topic of spectral analysis starting from an experimental approach to light diffraction.

 Online supplementary data available from stacks.iop.org/EJP/37/065701/mmedia

Keywords: optics, diffraction, optics education, Fourier transform

(Some figures may appear in colour only in the online journal)

1. Introduction

Coherent light that is partially obstructed by an object (sharp edges or tiny apertures), does not propagate as straight rays but along distinct angles and forms fringes on the observation

plane. Secondary schools and undergraduate students can easily appreciate that the fringe separation scales inversely with the size of the aperture [1]. However the quantitative study of diffraction is often limited by the uncertainty on the size of the diffractive elements: even high quality objects produced by photolithography or electron beam lithography [2] are affected by an intrinsic variability. Moreover, only very simple and regular patterns are available commercially for use in lab courses [3]. Diffraction experiments from every-day objects, such as those found in life science [4] and in electronics [5], have been recently proposed. Arbitrary patterns would be extremely useful in teaching physical optics basics but are difficult to obtain for low cost experiments [6].

The lack of basic calculus tools by undergraduate first year students additionally limits the efficacy of teaching units on this topic. There is an intrinsic complexity in the concept and use of waves and in their superposition. On the other hand, even at the level of the advanced undergraduate courses in optics, there is a wide misconception on the application of the Fourier transform (FT). Most of the time students have a theoretical knowledge of the FT, with no direct practical skills.

The typical situation in first year undergraduate courses and secondary schools is to organize lab demonstrations of the diffraction phenomenon with laser light impinging on regular patterns leaving the impression in the students that: (1) only narrow apertures produce non-straight propagation of light, (2) only regular patterns give rise to interference, (3) only light is affected by diffraction compared to other electro-magnetic and non-electromagnetic wave perturbations. During the undergraduate first year the theoretical introduction to diffraction often starts from the Huygens principle but the direct connection between diffraction and the mathematical tool of the FT is not drawn. This connection, particularly relevant in optics itself (image formation) and in a number of applied physics fields (electronics, radio communications), is often misunderstood by first year undergraduate students and seems to be out of reach for high school students.

Few pilot projects can be found on the internet that explore the possibility to work at the educational level on diffraction as a FT¹ [7] and [8]. An example is the spatial filtering lab modulus developed at the University of California at Santa Barbara (see footnote 1), in which spatial filtering was performed by small pieces of wires or meshes set in the lens focal plane. Other approaches discussed the diffraction from complex shapes, such as snow-flakes [8] or helices [7]. In particular, Lucas *et al* [7] simulated in the optical range the x-ray diffraction from the DNA helix by exploiting the size reduction of photograph slides [7]. Kits for high school students on Fourier optics have been developed by the pedagogical research of Waldorf schools [9] and are available on the internet.

We explore here the possibility to have a mixed laboratory–theoretical approach to diffraction that can help students, also through an interdisciplinary approach, to grasp the basic hypothesis that lie at its foundations and understand its connection to the FT. The proposed teaching unit should also support teachers in providing students with a direct view of the use of spectral analysis in various fields, from electronics (in one dimension) to optics (in two dimensions).

¹ University of California at Santa Barbara, ‘Spatial Filtering’, Lab course schematics for the Physics Department: <http://web.physics.ucsb.edu/~phys128/experiments/spatial/spatial.pdf>

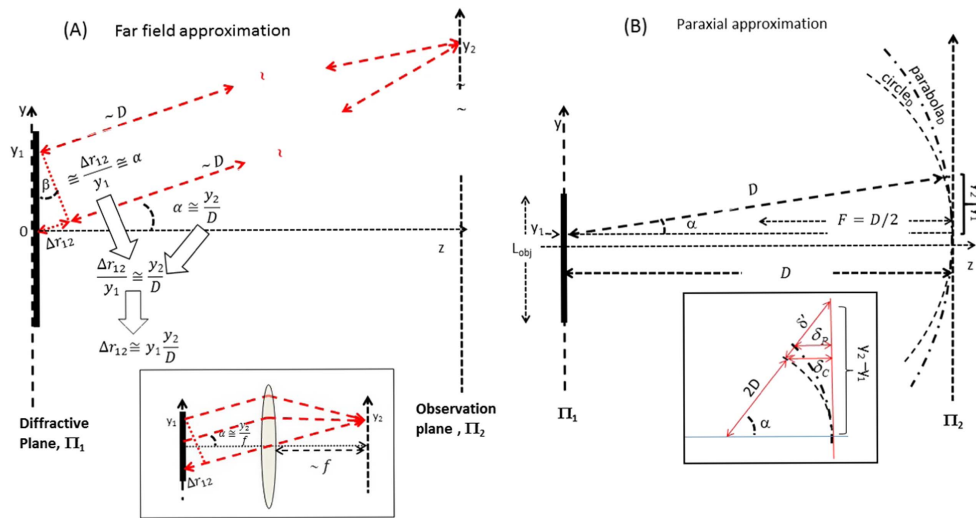


Figure 1. Diffraction from an aperture (projection on the z - y plane). (A) Far field (Fraunhofer) approximation. It is typically sketched without the lens that is necessary to obtain the far diffraction limit: we compare the path difference of two diffracted rays that are parallel due to the action of the lens. In this case the path difference depends on the product $y_2 y_1$ (notice that $\beta \cong \alpha$). The lower inset shows the ray tracing when a lens is used to collect light. (B) Paraxial (Fresnel) approximation: we compare the skewed ray (dashed line) with the un-deviated ray (parallel to the z -axis). r_{12} is the distance of a particular point $(x_1; y_1; 0)$ on Π_1 to a selected point on Π_2 plane $(x_2; y_2; D)$: $r_{12} = D + \delta'$. Since the deviation angle α is very small (not to scale in the figure), we can approximate δ' with δ_C , the deviation of Π_2 with respect to the circle of radius D (circle $_D$), and further approximate δ_C with δ_P , the deviation of Π_2 with respect to the parabola best approximating circle $_D$, that has a focus $F = D/2$ to the left of Π_2 . The discrepancy δ_P is then $\delta_P \cong \Delta y^2 / (4F) = \Delta y^2 / (2D)$.

2. Introducing FT by means of light diffraction

We exploit the commercially available microfiche printing technology for the construction of arbitrary patterns that can be used for diffraction experiments. This technology is based on photographic reproduction and reduction of the image on a support of cellulose acetate. It uses the silver halide process to create silver images and differs substantially from the Xerox-copying of photocopiers in which an electrostatic replica of the text is created on a drum. This approach allows students to study experimentally light diffraction and teachers to help students to discover its relation to the mathematical tool of the FT. Students can devise and build their own diffractive patterns by printing it on microfiches at very low cost. They can then compare the experimental diffraction patterns with those predicted according to the FT theory, therefore retrieving the basic properties of the FT while understanding the features of light diffraction.

This training module has been first tested and revised during laboratory sessions with high school classes visiting the educational laboratory LABEX at the University of Milano-Bicocca in the year 2014–15. It will be extended to first year undergraduate students during the 2017 academic year.

2.1. Where is the connection between diffraction and FT?

Prerequisites for the training module are a basic knowledge of the trigonometric functions, a description of the electric field as a plane and spherical wave, the concept of phase of a wave, the Huygens principle and the relation between our visual sensations and the field intensity (power per unit area), proportional to the square of the electric field. We assume that the light is monochromatic with wavelength λ (typically $\lambda \cong 0.5 \mu\text{m}$), wave vector $k = 2\pi/\lambda$ and angular frequency $\omega = 2\pi c/\lambda$.

The first approach to the relation between diffraction and the FT is based on the sketch in figure 1(A). The electric field impinging on the Π_1 plane is assumed to be a simple plane wave propagating along the optical axis, $E_1(x_1, y_1) = |A_1(x_1, y_1)| \cos[k_z z - \omega t]$. The amplitude $|A_1(x_1, y_1)|$ describes the transmission of the diffractive object and the incident field is uniform. We first imagine observing the image at *infinite distance* on Π_2 : the rays leaving different areas of the diffractive object on Π_1 are drawn as a parallel bundle leaving the diffractive object. This scheme, typically found in textbooks, poses two orders of logical problems in the students. First, the sketch is apparently nonsense because a parallel bundle of rays becomes, in the same picture, a focused beam on the observation screen. Second, smart students may ask whether the amount of energy collected on a screen at an infinite distance is enough to observe the diffraction pattern. Moreover, students may have already realized in a lab session that a clear diffraction pattern can also be observed at a finite distance. These issues pose a severe challenge for teachers to be solved with students at the conceptual level.

The answer to these concerns is the use of a lens (inset of figure 1(A)) set at the focal distance from the observation plane, Π_2 . The lens conveys then all parallel rays into small areas on the observation screen. The bundles of rays are focused on different positions on the diffraction (observation) plane, depending (almost linearly) on the angle between them and the optical axis. It is this very simple property, often overlooked by students and teachers, that makes the path difference between the propagating electric fields linear in their mutual distance, as sketched in figure 1(A). In analogy with the Huygens principle [10] we can then assume that the total electric field on the Π_2 plane will be the sum of all these wavelets and, referring to the definitions in figure 1(A), we can approximately write that

$$E_2^{(R)}(x_2, y_2) \approx \sum_{(x_1, y_1) \in \Pi_1} |A_1(x_1, y_1)| \cos \left[k \frac{x_1}{D} x_2 + k \frac{y_1}{D} y_2 - \omega t \right]. \quad (1)$$

Equation (1) reads: take the amplitude $|A_1(x_1, y_1)|$ of the field arising from on each point (or area) of the diffractive plane Π_1 , multiply it by a harmonic plane wave with k-vector $(k_x, k_y) = \left(\frac{2\pi x_2}{\lambda D}, \frac{2\pi y_2}{\lambda D} \right)$ (i.e. plane waves, but in the wave front plane!) and sum them over all the diffractive aperture. It gives a transformation rule between the two functions $E_2^{(R)}(x_2, y_2)$ and $|A_1(x_1, y_1)|$, that is proportional to the real form of the FT [10]. It is also important to notice that the use of equation (1) stands on the scaling rule between the Π_1 and the Π_2 coordinates through the definition of the spatial frequency vector, (k_x, k_y) .

For a direct comparison of equation (1) to the observed diffraction patterns we need to consider the effect of the parity of the diffractive object on the diffracted field. There is no reason to use a cosine function to describe the wavelets instead of a sine wave. By reasoning on the symmetry of these function ($\cos(x) = \cos(-x)$ and $\sin(x) = -\sin(-x)$), we can easily convince ourselves and students that diffractive patterns which are even in the coordinates will give diffracted fields described by equation (1), and that diffractive patterns which are odd in the coordinates will give diffracted fields described by a similar equation

$$E_2^{(I)}(x_2, y_2) \approx \sum_{(x_1, y_1) \in \Pi_1} |A_1(x_1, y_1)| \sin \left[k \frac{x_1}{D} x_2 + k \frac{y_1}{D} y_2 - \omega t \right]. \quad (2)$$

The field diffracted by a generic diffractive pattern, with no defined parity, will be given by the sum of equations (1) and (2). Since any light detector, our eye as well as the CCD camera of the students' smartphones, is sensitive to the intensity that is the average of the square of the electric fields, we can state that the diffracted light intensity is proportional to the sum of the two components, $E_2^{(R)}(x_2, y_2)$; $E_2^{(I)}(x_2, y_2)$ [2]

$$\begin{aligned} I(x_2, y_2) &\propto [(E_2^{(R)}(x_2, y_2))^2 + (E_2^{(I)}(x_2, y_2))^2] \\ E_2^{(R)}(x_2, y_2) &= \sum_{(x_1, y_1) \in \Pi_1} \cos(k_x x_1 + k_y y_1) A_1(x_1, y_1) \\ E_2^{(I)}(x_2, y_2) &= \sum_{(x_1, y_1) \in \Pi_1} \sin(k_x x_1 + k_y y_1) A_1(x_1, y_1). \end{aligned} \quad (3)$$

We have therefore written the intensity as the composition of two transforms of the original source distribution, $E_2^{(R)}(x_2, y_2)$; $E_2^{(I)}(x_2, y_2)$. For students of the last years of an undergraduate course, it should also be possible to recognize in these functions the real and imaginary parts of the same complex FT of $A_1(x_1, y_1)$. The limitation of this approach for first year undergraduate students or last year high school students may be that we purposely avoid using the complex number notation and choose to deal with the phases of the fields.

In all cases the relation between the FT transformation rule (equation (3)) and the observed pattern is straight forward if we know the behavior of the FT. Conversely, if we observe the behavior of the light diffracted by diffractive patterns of various shapes, we can infer the mathematical properties of the FT. This is the core message of the proposed training section.

2.2. Fourier transform black-box

In the proposed activity students gain first geometrically (figure 1(A)) the meaning of equation (2) and then compute the fast Fourier transform (FFT) of arbitrary patterns. The FT is taken as an operator: an input function, $g(x, y)$, with domain in the 2D space of plane Π_1 , enters the *black box* denoted $F[]$ and is modified in a new output function $F[g(x, y)] = \hat{g}(k_x, k_y)$, with domain in a 2D Fourier space, (k_x, k_y) . The scaling rule, $(k_x, k_y) = (kx_2/\lambda, ky_2/\lambda)$, allows us to cast the FFT spectrum onto the real observation space Π_2 . From the FT of a few basic functions and a few general transformation properties of the FT, students can qualitatively predict the diffraction profiles of arbitrary diffractive patterns, and compare them with observed profiles. For more complex profiles, numerical simulations can be performed either by means of freeware software for symmetric profiles that have real FT (for example ImageJ [11]), or of simple custom programs² in Python or Matlab, for asymmetric profiles for which both the cosine (equation (1)) and sine (equation (1)) components should be computed.

Table 1 summarizes the FT of a set of 1D functions that allows us to predict a wide variety of intensity patterns from 2D aperture profiles. A few important properties of the FT [12] help students to predict a variety of diffraction patterns starting from table 1.

The FT linearity property mathematically states the superposition principle of the electromagnetic field. From the optical point of view, a diffractive pattern composed as the

² A Python code that can be used to compute the 2D diffraction profile can be downloaded from the following link: <https://drive.google.com/open?id=0B8B9d2LsyXlcfjRyWmo3LUwyemNLWFphStfQzIGcGt2Y0tDb1Jad05VQzdyODhqbWR55ekE>

Table 1. Fourier transform of useful profiles.

$g(x)$	$\hat{g}(\xi)$
$\text{rect}_{r_0}(x) = \begin{cases} 1 & x < r_0 \\ 0 & x \geq r_0 \end{cases}$	$r_0 \text{sinc}(2r_0\xi)$
$\text{circ}_{r_0}(x, y) = \begin{cases} 1 & x^2 + y^2 < r_0^2 \\ 0 & x^2 + y^2 \geq r_0^2 \end{cases}$	$\pi r_0^2 \text{somb}(r_0\xi)$

Fourier transform, $F[g(x)] = \hat{g}(\xi) = \frac{1}{2\pi} \int_{-\infty}^{+\infty} dx g(x) \cos[2\pi\xi x]$, of two basic functions. The Fourier variables are ξ and η . The $\text{sinc}()$ function is defined as $\text{sinc}(\xi) = \sin(\pi\xi)/(\pi\xi)$. The $\text{somb}(r)$ function can be seen as a generalization of the $\text{sinc}()$ function in the radial coordinate. It is defined as $\text{somb}(r) = 2J_1(2\pi r)/(2\pi r)$, where $J_1(2\pi r)$ is the first order Bessel function, and an exemplary plot is reported in figure 5(B), left inset.

superposition of two patterns will produce a diffraction profile that is the sum of the diffraction profiles of the two individual diffractive patterns. Analytically we can write

$$F[\alpha g(x) + \beta f(x)] = \alpha \hat{g}(k_x) + \beta \hat{f}(k_x) \text{ linearity} \quad (4)$$

where α and β are coefficients. The FT scaling property states that a geometric expansion on the diffractive patterns will produce a contraction in the diffractive profiles. This is the mathematical formulation of the observation that fine structures in the diffractive plane give rise to widely separated fringes in the diffraction profiles and can be written as

$$F[g(bx)] = \frac{1}{b} \hat{g}\left(\frac{k_x}{b}\right) \text{ scaling.} \quad (5)$$

Shifting the spatial variable results instead in the multiplication by an oscillating factor in the frequency domain. If we combine the shifting with the linearity property and take into account that the observed intensity is (proportional to) the square modulus of the FT, we can write that

$$|F[g(x) + g(x \pm a)]|^2 = 2(1 + \cos(k_x a)) |\hat{g}(k_x)|^2 \text{ shifting.} \quad (6)$$

Equation (6) states that if we build a diffractive pattern as the superposition of two shifted (by $dx = a$) replicas of the same diffractive pattern, the resulting diffraction (intensity) profile is the original diffraction pattern modulated by fringes with the wavelength $\Lambda = D\lambda/a$, (figure 1) scaling inversely with the spacing a . We can extend this property to a collection of many $(2N + 1)$ replicas of equally spaced (spacing = d) identical diffractive elements $f(x)$

$$f_{\Sigma}(x) = \sum_{i=-N}^{i=+N} f(x - id). \quad (7)$$

This case can deal in general with the so called convolution theorem (of which we do not give the general formulation here) that allows us to write [12] the diffracted field as the product of the original diffracted pattern times a multi-periodic function

$$F[f_{\Sigma}(x)] = \hat{f}(k_x) \left(1 + 2 \sum_{i=1}^N \cos(k_x di) \right) \text{ sampling.} \quad (8)$$

Equation (8) can be derived from the application of the shifting and linearity property and implies that the FT of the grating is the FT of the single slit multiplied by a complex harmonic modulation factor. We will apply equation (8) for a finite ($N \cong 10$) number of replicas, in contrast to most text books [10, 12]. Finally we notice that the diffraction patterns are often described by separable functions of the coordinates on the diffraction plane. In this case we

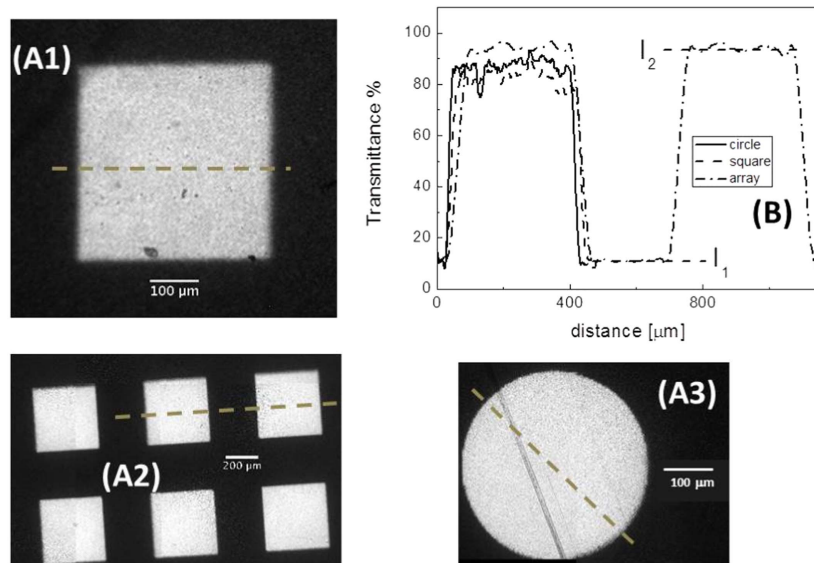


Figure 2. Exemplary transmission confocal images of a square diffraction pattern (A1), of an array of squares (A2) and of a circle (A3), printed on microfiches. Plot (B) reports the transmission signal measured along the straight lines showed superimposed to the transmission images (gray dashed lines).

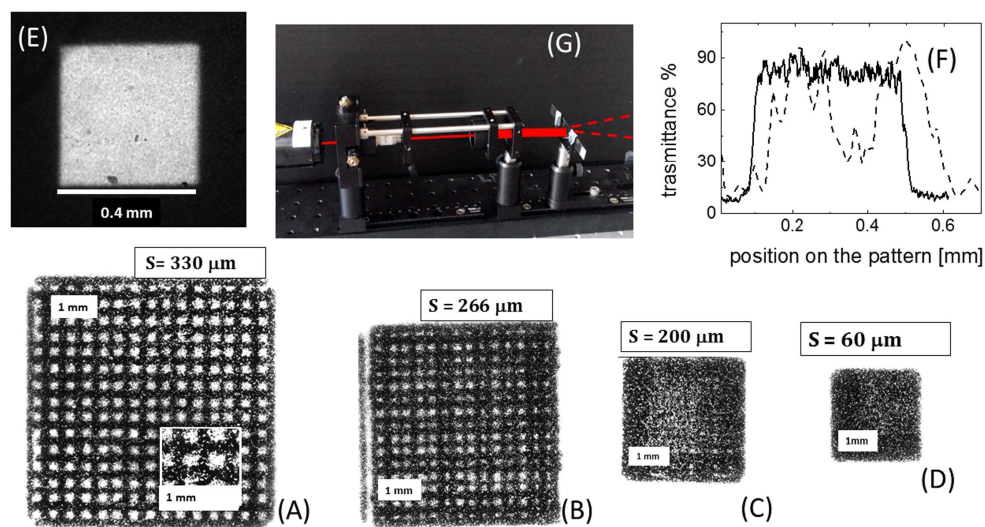


Figure 3. Comparison of Xerox-printed (panels (A)–(D)) to microfiche printing (panel (E)). The white bars report the linear size in each panel or blow up (as in panel (A)). Panels (A)–(D) are printed rectangular arrays with spacing $330 \geq S \geq 60 \mu\text{m}$. Panel (E) is a $400 \times 400 \mu\text{m}^2$ square aperture printed on a microfiche. Panel (F) reports the profiles of the square aperture (panel (E)) and of two periods of the $S = 330 \mu\text{m}$ rectangular array (panel (A)) as solid and dashed lines, respectively. Panel (G) is a photo of the laser and microfiche holder setup.

can simply compute independently the transforms over the two axes

$$\begin{cases} f(x, y) = g(x)h(y) \\ F[f(x, y)] = \hat{g}(k_x)\hat{h}(k_y) \end{cases} \quad \text{separability.} \quad (9)$$

This property will allow us to refer to table 1 when dealing with 2D diffractive patterns that can be described by the product of two 1D profiles.

3. Examples

The diffraction patterns were drawn (Draw, OpenOffice™) as black profiles on a white background (A4 page size, 400 dpi resolution, 21×30 cm, 23 times reduction). The typical linear size of the apertures on the A4 page is 1 cm, which corresponds on the microfiches to a linear size $\approx 430 \mu\text{m}$. The spatial resolution on the microfiches was $11 \pm 2 \mu\text{m}$, as estimated from the sharpness of the boundary profile measured by confocal transmission microscopy (SP5, Leica Microsystems, transmission mode). The transmittance was estimated by dividing the pixel content by the dynamic range (255) of the image (figure 2, panels A1 and B). The S/N ratio was computed as $S/N = I_2/I_1$, where I_2 and I_1 are the transmission signal collected in the bright and the dark regions, respectively, of the diffractive patterns. The average value is $S/N = 8 \pm 0.6$.

By comparison, direct Xerox-printing on acetate substrates at 1200 dpi provides in principle only $22 \mu\text{m}$ resolution. Moreover, the Xerox-printing on acetate sheets is intrinsically less accurate. The optical transmission microimaging of diffractive patterns obtained by Xerox-printing, reported in figures 3(A)–(D), compared to the one obtained on a microfiche (figure 3(E)) indicates that details smaller than $220\text{--}240 \mu\text{m}$ cannot be realized with good S/N (figure 3(F)). It is likely that the electrostatic toner transfer produces spurious dots on the slide that severely affect the S/N ratio ($S/N \cong 3.5 \pm 1.9$; figure 3(F)) and the sharpness of the patterns with details smaller than $300 \mu\text{m}$.

The conventional microfiche printing provides the negative of the original drawing: we obtain therefore transparent apertures on a dark background. The transmittance of the background is $11 \pm 2\%$ compared to that of the apertures that is $87 \pm 9\%$ (see the discussion of figure 2). The microfiches were read by means of an extremely simple and low cost setup. A He–Ne laser beam ($\lambda = 0.633 \mu\text{m}$, power 5 mW, Melles-Griot, USA) passes through a $4\times$ beam expander (two lenses with focal lengths $f_1 = 10$ mm and $f_2 = 40$ mm set at a distance $d = f_1 + f_2$) to obtain a uniform beam ≈ 5 mm in diameter that is diffracted by the microfiche (figure 3(G) and the supplementary material (SM), ‘Sketch of the optical setup’, figure SM1). Snapshots of the diffraction patterns were taken on a screen $D = 1.5$ m away from the microfiche by means of a smartphone digital camera³. The laser beam was not spatially filtered. A hole (with a radius $r \approx 8$ mm) was cut at the center of the screen in order to get rid of the bright central spot. The hole shadows all the spatial frequencies smaller than $1/(200\lambda)$, which corresponds to details on the sample with angular size ≤ 5 mrad.

We devised and tested a series of diffraction patterns printed on microfiches that should allow students to explore the basic FT theorems outlined above (equations (4)–(9)). Numerical simulations of the expected pattern can be performed using a Python program (see footnote 2), and qualitative theoretical predictions can be made from equations (4)–(9).

³ We employed a smartphone camera. A sharpening mask was applied to the images reported in the figures. Please note that the naked eye observation offers a better on-field visualization of the diffraction patterns.

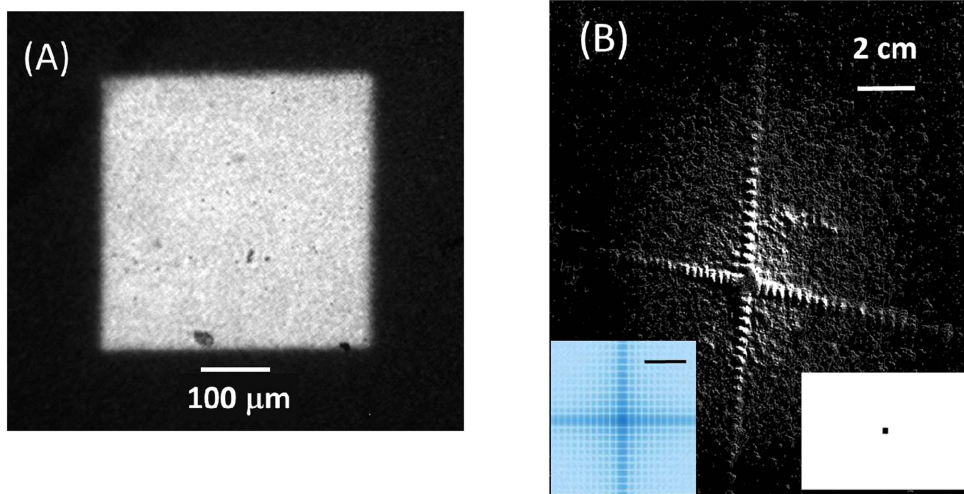


Figure 4. (A) Square diffraction pattern on the microfiche as detected by confocal transmission microscopy. (B) Screen shot of the optically generated diffraction pattern measured at $D = 1.5$ m from the microfiche. The lower left inset shows the numerically simulated diffraction pattern (no noise added, bar = 2 cm). The lower right inset shows the square pattern printed on the A4 size page.

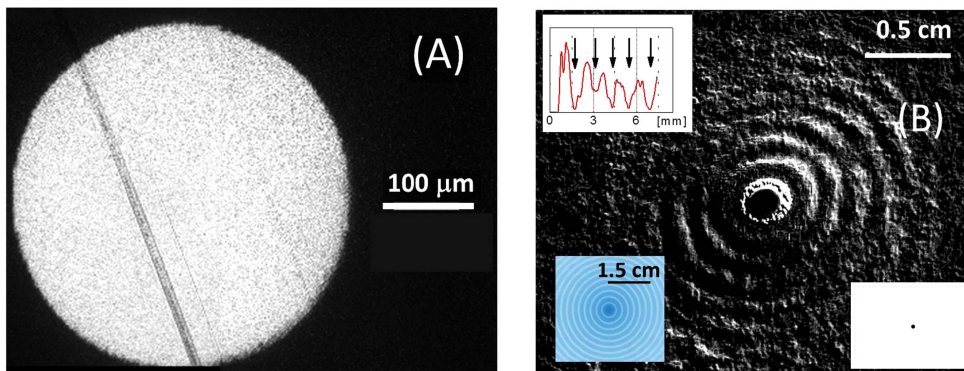


Figure 5. Circular diffraction pattern. (A) Circular pattern printed on the microfiche as detected from confocal transmission microscopy. (B) Screen shot of the optically generated diffraction pattern measured at $D = 1.5$ m from the microfiche. Lower right inset: diffractive element to be printed on the microfiche. The size of the page is A4. Lower left inset: numerically simulated diffraction pattern (no noise added). The upper left inset reports the average profile along the radial coordinate on the diffractogram. The vertical arrows indicate the zeros of the $somb(x)$ function as discussed in the text.

3.1. Square aperture (separability)

The function that models this aperture is

$$r(x, y) = \text{rect}\left(\frac{x}{b}, \frac{y}{b}\right) = \text{rect}\left(\frac{x}{b}\right)\text{rect}\left(\frac{y}{b}\right) \quad (10)$$

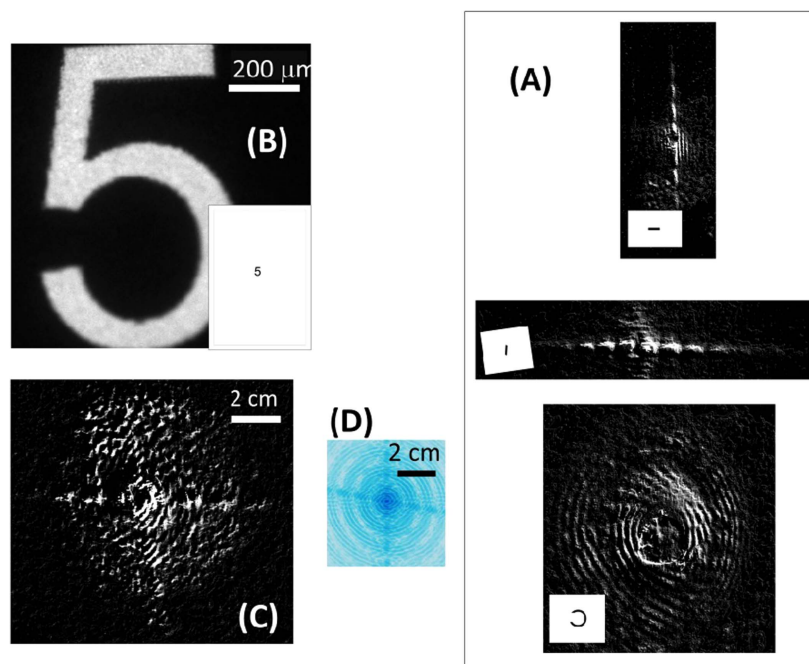


Figure 6. Linearity of the FT. (A) Snapshots of the diffraction patterns obtained from the individual diffractive patterns (horizontal dash, vertical dash and inverted 'c') used to build the '5' shape diffractive pattern. The panels on each snapshot are the corresponding diffractive patterns: the paper size is not in the A4 scale for display purposes. (B) Diffractive pattern (symbol '5') on the microfiche as detected from confocal transmission microscopy. The inset is the corresponding diffractive pattern (A4 size). (C) Screen shot of the optically generated diffraction pattern measured at $D = 1.5$ m from the microfiche. (D) Numerically simulated diffraction pattern (no noise added).

where b is the full width of the square aperture, $b = 385 \pm 10 \mu\text{m}$. The analytical FT is a sinc () function in the FT variables $(\xi, \eta) = (x_2/(\lambda D), y_2/(\lambda D))$. According to the separability property (equation (9)) we can write the FT of equation (10) as

$$\hat{r}(\xi, \eta) = \frac{1}{b^2} \text{sinc}\left(\frac{x_2 b}{\lambda D}\right) \text{sinc}\left(\frac{y_2 b}{\lambda D}\right). \quad (11)$$

On the recorded diffractogram (figure 4(A)), we can appreciate the presence of the two sinc() functions that intersect each other at the center of the diffraction image on the screen. This feature can be retrieved on the simulated pattern (figure 4(B), lower left inset). The fringe spacing can be computed from the number of zeros observed within a linear size = 40 mm, averaged over the two symmetry axes. We measure a fringe spacing ≈ 2.7 mm, in very good agreement with the expected value $D\lambda/b = 2.6 \pm 0.6$ mm, which is the first zero ($x = 1$) of the sinc(x) function ($D = 1.5 \pm 0.02$ m).

Table 2. Airy function zeros.

Zero position [mm]	$(j_{n+1}/j_n)_{(exp)}$	$(j_{n+1}/j_n)_{(Airy)}$
1.62 ± 0.06		
3.1 ± 0.06	1.8 ± 0.2	1.8
4.1 ± 0.06	1.4 ± 0.1	1.45
5.2 ± 0.06	1.3 ± 0.1	1.31
6.6 ± 0.06	1.2 ± 0.1	1.24

Analysis of the position of the minima in the diffractogram obtained from the circular aperture (see figure 5). The position of the minima are indicated as $\{j_n\}_{n=1,2,\dots}$. The ratio of these positions can be taken as a good measure of the shape of the Airy function.

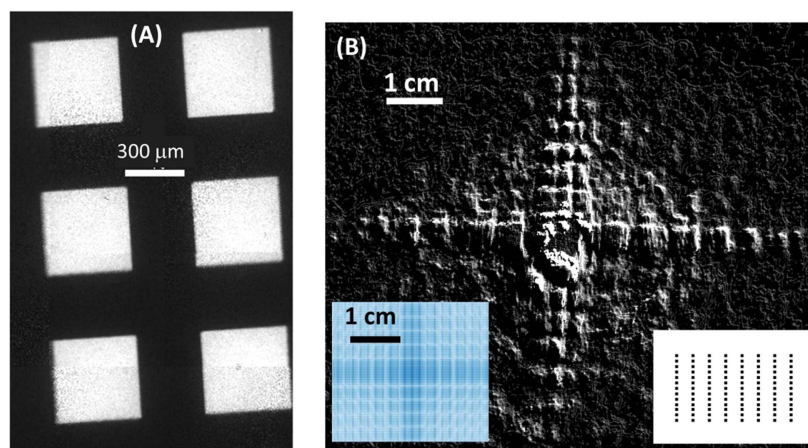


Figure 7. Diffraction pattern used to test the convolution properties of the FT. (A) Confocal transmission microscopy image of the rectangular array of square apertures. (B) Screen snapshot of the optically generated diffraction pattern measured at $D = 1.5$ m from the microfiche. Lower right inset: the square regular array to be printed on the microfiche substrate (A4 paper size). Lower left inset: numerically simulated diffraction pattern (no noise added).

3.2. Circular aperture (Airy disc)

The diffraction pattern of a circular aperture has the shape of the Airy function ($\text{Airy}(x) = \text{somb}^2(x)$, table 1 and figure 5(B), left inset). The diffractive pattern has a diameter $= 370 \pm 5 \mu\text{m}$ as imaged by confocal transmission microscopy (figure 5(A)). At the observation distance $D = 1.5$ m, the first minimum falls at ≈ 1.62 mm from the center of the diffractogram. It is noteworthy that the higher order zeros are not equally spaced (inset of figure 5(B)), in agreement with the shape of the Airy function (table 2).

3.3. Number 5 (linearity)

We have investigated the superposition principle on a composite pattern, the symbol ‘5’, whose building blocks are two $\text{rect}()$ functions and a ‘C’ mirrored through a vertical line (figure 6(A)). The measured diffraction patterns are two orthogonal $\text{sinc}(x)$ functions and one $\text{Airy}(x) = \text{somb}^2(x)$ function (figure 6(A)). The diffraction pattern generated from the symbol ‘5’ printed on the microfiche (figure 6(B)) shows a slanted cross shape superimposed on a set

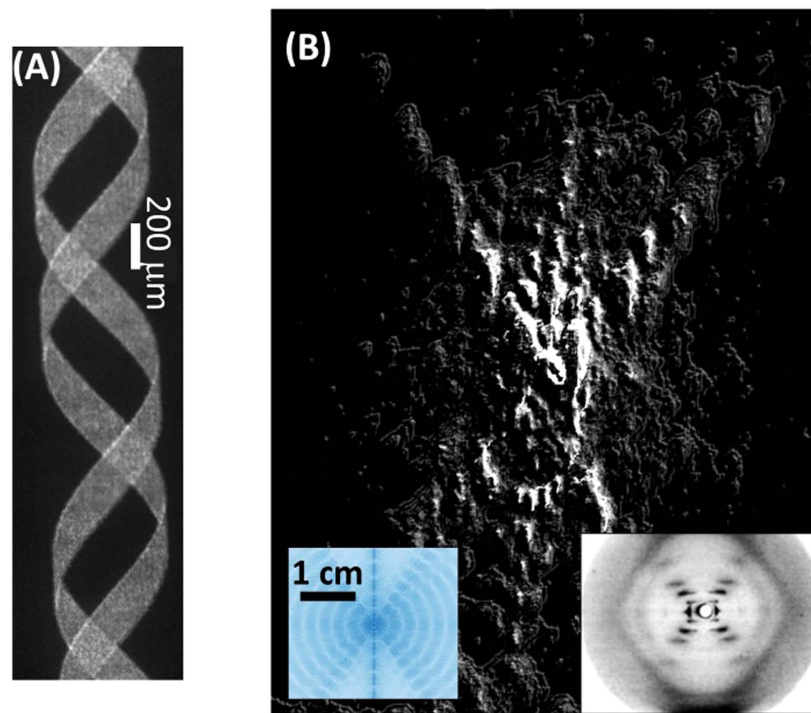


Figure 8. Diffraction pattern used to replicate the Franklin–Gosling experiment on DNA. (A) The 2D projection of the DNA helix printed on the microfiche (confocal transmission microscopy). (B) Screen snapshot of the optically generated diffraction pattern measured at $D = 1.5$ m from the microfiche. The lower right inset reproduces the famous x-ray diffractogram from aligned DNA fibers. The lower left inset reports the numerically simulated diffraction pattern (no noise added).

of concentric rings (figure 6(C)). This pattern can indeed be obtained as the linear combination of the FT spectra reported in figure 6(A), and is confirmed by the numerical simulations (figure 6(D)). Although the diffraction rings cannot be discerned clearly in the diffraction pattern (figure 6(C)), the slanted cross is clearly visible.

3.4. Sampling and convolution

This FT sampling property (equation (8)) is more easily analyzed directly on the diffractive pattern than studied on the analytical expression. A regular rectangular array of square apertures printed on a microfiche (figure 7(A)) produces the diffraction pattern reported in figure 7(B), which is in close agreement with the prediction (figure 7(B), lower left inset). If we compare figure 4(B) to figure 7(B), the presence of the complex harmonic modulation factor (see equation (8)) in the measured pattern is evident. The diffraction pattern is that of a single square slit, a double sinc() pattern, which is sampled regularly by the comb function as predicted by the FT sampling property (equation (8)).

3.5. DNA diffraction

X-ray diffraction (wavelength ~ 0.2 nm) was employed by Rosalind Franklin and Raymond Gosling [13] in 1952 to investigate the structure of DNA (linear scale ~ 1 nm). The

interpretation that Watson and Crick gave of the x-ray diffractive pattern was largely qualitative and based on the general properties of the FT: finely spaced regular arrays give a diffraction pattern with widely spaced diffraction maxima (scaling theorem, equation (5)). The Franklin–Gosling experiment was carefully replicated by Lucas *et al* [7] in the optical domain by exploiting the photographic reduction of slides. These authors simulated a fiber of helices with axis perpendicular to the diffracted light and discussed also the (minor) effect of the 2D projection of the helix onto a plane that contains the cylindrical axis. Here we show that a clearly discernible diffraction pattern can be obtained from microfiches reporting a transparency function that is the 2D projection of a single DNA double helix structure (figure 8(A)).

The diffractive pattern (figure 8(A)) does not reproduce the details of the DNA base pairs. Therefore both the simulated and measured diffraction patterns do not reproduce all the details visible in the x-ray diffractogram (figure 8(B), inset). However the characteristic X-shape can be recognized on the measured diffraction pattern (figure 8(B)) and the ladder structure that arises from the helix pitch is visible.

4. Applications

We briefly describe the proposal of a basic version of the learning unit to high school students who attended the LABEX laboratory during a 10 day stage at the University of Milano-Bicocca in spring 2016. Students from the last year of high school with scientific bachelor were divided in two 5–7 student groups. First an introduction was given to the concept of base in algebra and in 2D and 3D vector algebra through the use of the unitary vectors (\hat{i} , \hat{j} , \hat{k}) along the three orthogonal axes of a Cartesian system of reference. Then we moved to the direct observation, starting with a short description of the setup and the observation of the diffractive patterns from simple geometries (dots, squares). Only geometrical optics concepts were used at this stage. The students were shown the original enlarged diffractive patterns on A4 paper sheets and a discussion among their peers about the symmetry of the diffractive pattern and that of the diffraction pattern was stimulated. Most students were initially refractory to this qualitative approach (see the SM, ‘Typical activity on the diffractive microfiche plates’). It must be noted that the observation of the patterns was done more easily by eye and their recording was done by sketching them in a lab book. The recording of the patterns with a CCD camera, for example a smartphone, is more difficult and requires some image processing, at least an ‘edge enhancer’ filter. This was done by the tutors when there was the need to build a record of the activity.

The second stage of the learning unit consists in a brief introduction to the diffraction process in order to come to equation (3). As stated in section 3, this requires some pre-knowledge about the Huygens principle, at least in its very general and qualitative statement. During the discussion, equation (3) is compared to the expression of a number in different bases, a concept that should be more familiar to students and would help them in understanding the use of a set of basis functions.

The third step of the basic learning unit we proposed deals with an example of a quantitative observation of the diffractive patterns. This has been done in particular by comparing the diffractive patterns from single circles (see figure 5 and table 2) and the theoretical prediction expressed in terms of the Bessel function. The digitization of the diffractive patterns and analysis with the ImageJ [11] tools involved the application of an enhance filter and the extraction of six radial profiles from the image. The profile shown in

figure 5 is obtained by averaging these measurements once they have been shifted along the radial position to best superimpose the profiles.

A second quantitative example was related to the superposition principle and was based on the ‘number 5’ example (see figure 6). The proposal ended with a hands-on session in which the students were observing the diffraction patterns from microfiche patterns reporting single letters and inferring the letter from it, according to the superposition of the diffraction patterns of elementary elements (circles, squares, lines) observed previously.

Attendance at the learning unit should be followed by a short form that evaluates the skills and knowledge acquired by the students. We have set up a preliminary version of this form (Google Form utility) and shared it with the students. This evaluation form is reported in the SM (‘Web-form for the post-evaluation of the learning unit’) together with a short analysis of the survey. This survey, though administered to a restricted number of students, indicates that the most deeply acquired skills relate to the recognition of the diffraction pattern as a superposition of basis diffractive patterns. This is not unexpected because this skill was mainly acquired in the hands-on (third) part of the learning unit. The revision of the form and its administration to a larger set of students (LABEX is typically attended by 350–400 high school students per academic year) is scheduled for the next academic year.

5. Discussion

Though the proposed learning unit is specifically devoted to first year undergraduate and last year high school students, sophomore or junior undergraduate students may also take advantage of the proposed experimental approach. In this case, in fact, they should master the FT as a mathematical tool. However they typically lack comprehension of its physical meaning and use. Moreover, from the theoretical optics point of view, some confusion may arise in these students about the connection between the vision of the propagating far field as a FT, i.e. a superposition of plane waves *in the 2D phase wave plane*, and the vision provided by the Huygens principle in terms of superposition of spherical wavelets *in 3D space*. The fact that these two visions look very similar and are indeed closely related, but not identical, is not often recognized by students, even those in the second or third year of undergraduate courses. In fact, the two descriptions agree if we write the Huygens principle in terms of the FT with the appropriate approximations. We offer here a simple geometrical argument of this connection that can be proposed to undergraduate sophomore/junior students after the experimental unit.

According to the Huygens principle, the field $E_2(\vec{r}_2, t)$ propagated at the point \vec{r}_2 is the sum of spherical wavelets, $\Delta x_1 \Delta y_1 |A_1(x_1, y_1)| \cos[kr_{12} - \omega t - \pi/2]/r_{12}$, each arising from a small area, $\Delta^2 \vec{r}_1 = \Delta x_1 \Delta y_1$, on the aperture plane Π_1 (see figure 1(B)) with the same amplitude and initial phase as the origin field $E_1(x_1, y_1)$ but in quadrature with it

$$E(x_2, y_2, D) = \sum_{(x_1, y_1) \in \Pi_1} \frac{\cos[kr_{12} - \omega t - \pi/2]}{\lambda r_{12}} |A_1(x_1, y_1)| \Delta x_1 \Delta y_1. \quad (12)$$

The electric field $E_1(x_1, y_1)$ acts as a transparency function that modulates in amplitude spherical wavelets with the function $|A_1(x_1, y_1)|$, which describes the shape of the diffractive pattern. The distance between the wavelet center and the observation point is $r_{12} = |\vec{r}_{12}| = |\vec{r}_2 - \vec{r}_1|$ which can be written as $r_{12} = \sqrt{D^2 + \Delta \rho^2}$, where $\Delta \rho^2 = (x_2 - x_1)^2 + (y_2 - y_1)^2$. In order to retrieve the linear dependence of the phases with the coordinates on the diffractive plane, we need to apply two successive approximations. The first, *paraxial* (or *Fresnel*), amounts to approximate the difference

between the object plane Π_2 and a sphere of radius D , with the paraboloid that best fits the sphere (see figure 1(B)). This process leads to the linearization of the optical path $kr_{12} \cong kD + k\frac{\Delta\rho^2}{2D}$. It can be shown analytically that this approximation is valid for

$D \gg \sqrt[3]{L_{\text{DIFF}}^4/\lambda}$, that implies $D \gg 30$ cm for a size of the diffraction pattern $L_{\text{DIFF}} \cong 1$ cm.

The paraxial approximation of the optical path still does not bring us to the FT of the diffractive element because it contains a quadratic form $k\Delta\rho^2/2D$, composed of three terms. The quadratic term $kr_2^2/2D = k(x_2^2 + y_2^2)/2D$ counts as a constant phase in equation (12) and can be disregarded. A second quadratic term $kr_1^2/2D = k(x_1^2 + y_1^2)/2D$ should instead be summed up in equation (12), raising a difficult calculus issue. Most textbooks introduce at this stage the *Fraunhofer* approximation: $kr_1^2/2D \cong kL_{\text{OBJ}}^2/2D \ll \pi$, where the diffractive element size $L_{\text{OBJ}} \cong 1$ mm. Since the size of the diffractive pattern is typically $L_{\text{OBJ}} \cong 2$ mm, this condition is more severe than the Fresnel condition, $D \gg 2$ m. In this condition we are left with the cross-term $k(x_1x_2 + y_1y_2)/D$ that looks actually like a Fourier kernel, since it is linear in the coordinates of the Π_1 plane. The Fraunhofer limit, $D \gg 2$ m, is geometrically equivalent to collecting parallel rays from the diffractive plane (see figure 1(A)) and therefore to using a lens for the observation of the diffracted field.

6. Conclusions

In conclusion we have shown that inexpensive microfiche technology can be used to explore experimentally light diffraction and its close connection with the mathematical tool of the Fourier transform. The cost of microfiche printing in a public copying center is approximately 0.15€ per diffraction pattern (or A4 sheet). We suggest that there is no real need for a university lab or department to own a microfiche printer.

The learning approach described here has been developed for last year high school or first year undergraduate students, who do not yet have knowledge of the FT as an analytical tool. The key feature of the learning unit is to offer these students the possibility to produce arbitrary 2D diffractive patterns. In this way students can actively plan a study of the light diffraction and actually visualize the basic properties of the FT in 2D space (as an alternative to the 1D approach of electronics). The building method and the learning unit on the FT were tested and refined on last year high school students visiting the educational lab LABEX of the University of Milano-Bicocca in the year 2014–15.

We should finally consider that sophomore and junior undergraduate students, who should have theoretical knowledge of the FT as an analytical tool, rarely have a clear concept of the physical meaning and implications of the FT analysis. The possibility to develop arbitrary diffractive patterns could then be advantageously exploited by these students to fill this gap.

References

- [1] Gan K and Law A T 2009 Measuring slit width and separation in a diffraction experiment *Eur. J. Phys.* **30** 1271
- [2] Groeber S, Vetter M, Eckert B and Jodl H-J 2014 Diffraction and interference—a standard teaching topic using non-standard diffracting objects *Eur. J. Phys.* **35** 015003
- [3] Fischer R 2012 Teaching diffraction with hands-on optical spectrometry *Phys. Educ.* **47** 603
- [4] Groff J R 2012 Estimating the size of onion epidermis cells from diffraction patterns *Phys. Teach.* **50** 420

- [5] Barreiro J J, Pons A, Barreiro J C, Castro-Palacio J C and Monsoriu J A 2014 Diffraction by electronic components of everyday use *Am. J. Phys.* **82** 257
- [6] Slogoff H, Mackowiak J, Shishkov M and Johnson A T 2004 Photolithographic fabrication of diffraction and interference slit patterns for the undergraduate laboratory *Am. J. Phys.* **72** 1328
- [7] Lucas A A, Lambin P, Mairesse R and Mathot M 1999 Revealing the backbone structure of B-DNA from laser optical simulations of its x-ray diffraction diagram *J. Chem. Educ.* **76** 378
- [8] Puang-Ngern S and Almeida S P 1985 Converging beam optical Fourier transforms *Am. J. Phys.* **53** 762
- [9] <http://lehrerseminar-forschung.de/shop/geraete/physik/optische-filterung-hausbild.html>
- [10] Klein M V and Furtak T E 1986 *Optics* 2nd edn (New York: John Wiley & Sons) pp 337–99
- [11] <http://imagej.nih.gov/ij/>
- [12] Meikle H D 2004 *A New Twist to Fourier Transforms* (Weinheim: Wiley-VCH) pp 34–6
- [13] Franklin R E and Gosling R G 1953 Evidence for 2-chain helix in crystalline structure of sodium deoxyribonucleate *Nature* **172** 156